Synthetic and Systems Biotechnology 10 (2025) 751–763

Contents lists available at ScienceDirect

Synthetic and Systems Biotechnology

journal homepage: www.keaipublishing.com/en/journals/synthetic-and-systems-biotechnology

Original Research Article

iCASRED, a scarless DNA editing tool in *E. coli* for high-efficiency engineering of natural product biosynthetic gene clusters

Guosong Zheng [a], Jiafeng Xu [a], Hewei Liu [a], Huimin Hua [a], Andrei A. Zimin [b], Wenfang Wang [a,*], Yinhua Lu [a,**]

[a] College of Life Sciences, Shanghai Normal University, Shanghai, 200234, China
[b] G.K. Scriabin Institute of Biochemistry and Physiology of Microorganisms RAS, Pushchino, 142290, Russia

ARTICLE INFO

Keywords:
CRISPR-Cas9
Scarless gene cluster editing
E. coli
Actinomycete-derived natural products

ABSTRACT

Efficient gene cluster editing tools are one of the key techniques for discovering novel compounds encoded by silent natural product (NP) biosynthetic gene clusters (BGCs) in microbial genomes. Currently, *in vivo* BGC editing tools developed in *E. coli* is the most widely used, but they often introduces DNA scars into gene clusters, which may affect the function of target NP BGCs. Herein, a genome-integrated Cas9/λRed system-based *in vivo* scarless gene cluster editing tool (iCASRED) was established in *E. coli* BL23, which was constructed on the basis of BL21/DE3 with *recA* deletion and simultaneous integration of an inducible sgRNA targeting the editing plasmid (an all-in-one plasmid with the BGC-targeting sgRNAs and repair templates). iCASRED achieved scarless editing of single targets in three tested gene clusters (44.2, 72.0, and 76.2 kb) cloned in either a single-copy BAC plasmid or a high-copy plasmid pCAP01 with the efficiencies of 28.8 % ± 3.9 %–100 % ± 0 %. Furthermore, this tool could enable convenient, high-efficiency iterative editing. Finally, we achieved 24.4 % ± 3.8 % efficiency for simultaneous double-target editing by replacing Cas9 by nCas9 ($Cas9^{D10A}$). Collectively, iCASRED provides a simple, convenient, and cost-effective approach for engineering gene clusters, which may facilitate the discovery of novel NPs and strain improvements for high-yield of target compounds.

1. Introduction

Natural products (NPs) isolated from actinomyetes have been one of the most abundant sources of novel lead chemical compounds for the development of therapeutic agents, such as antitumor drugs, biopesticides, and immunosuppressants, etc [1–3]. However, strain improvements for high-yield of many target NPs in native hosts were hampered by the difficulties in cultivating or lack of effective genetic manipulation tools. In addition, with the advances in microbial genome sequencing and bioinformatics tools, a huge number of NP biosynthetic gene clusters (BGCs) has been predicted to be encoded in actinomycete genomes with an average of approximately 20–30 NP BGCs in each genome, which are considered as untapped treasure for novel bioactive NPs discovery [3–5]. Unfortunately, most BGCs are cryptic or silent under normal laboratory culture conditions. To address the above issues, an effective strategy is to express these target BGCs in compatible heterologous actinomycete hosts with mature and convenient fermentation process and genetic manipulation tools [6–8].

To facilitate heterologous expression of NP BGCs, it is always necessary to edit or refactor the BGCs, which could detach the expression of BGCs from complex natural regulation, thereby overcoming transcription silence [9,10]. Nowdays, a growing number of BGC editing tools are being developed, which could be mainly divided into two categories: *in vitro* and *in vivo* editing tools [9,11,12]. Two novel *in vitro* editing tools by coupling RNA-guided Cas9 endonuclease with T4 DNA polymerase or Gibson assembly were established [13–15], which have provided effective methods for refactoring BGCs. *In vivo* technologies were established in *E. coli* or *Saccharomyces cerevisiae* based on DNA homologous recombination. In *E. coli*, Red/ET Recombineering-based genome editing tools based on the recombinases RecE/RecT from the Rac prophage or Redα/Redβ from the lambda phage were extended for editing BGCs, which enables high-efficiency promoter refactoring or

Peer review under the responsibility of Editorial Board of Synthetic and Systems Biotechnology.
* Corresponding author.
** Corresponding author.
E-mail addresses: wangwenfang@shnu.edu.cn (W. Wang), yhlu@shnu.edu.cn (Y. Lu).

https://doi.org/10.1016/j.synbio.2025.03.008
Received 4 March 2025; Received in revised form 18 March 2025; Accepted 19 March 2025
Available online 20 March 2025

domains/modules exchange [9,16–19]. In *S. cerevisiae*, a series of efficient gene cluster editing tools have been developed using transformation-associated recombination (TAR) [18,20] or combined with Cas9, including mCRISTAR [21] and mpCRISTAR [22], which enabled high-efficiency simultaneous replacement of up to eight promoter cassettes. However, the above BGC editing or refactoring tools have some obvious shortcomings that hinder their wide applications. *In vitro* approaches and *in vivo* Red/ET Recombineering tools in *E. coli* are time-saving and cost-effective, but they can only be employed for editing single targets in BGCs (e.g. deletion or insertion of single genes or replacement of single promoters). Moreover, scars like antibiotic selection markers or restriction enzyme sites are left at editing sites. Just recently, a novel *in vivo* editing tool in *E. coli*, CRISTER, integrating RecET with Cas9, has been developed, which could achieve high-efficiency multiplexed gene cluster refactoring (promoter replacements) [23]. However, at least one selection marker still needs to be inserted into BGCs for multiplexed refactoring. For yeast TAR-based tools, they are cumbersome and time-consuming, due to the slow growth and the involvement of complicated protoplast preparation/-transformation. Furthermore, to achieve multiplexed promoter engineering, at least one autotrophic marker is required to insert into the promoter cassettes.

In this study, based on the CRISPR-Cas9 genome editing tool in *E. coli* [24], a genome-integrated Cas9/λRed system for *in vivo* scarless NP BGC editing was established using BL21/DE3 as the chassis. Through chassis modification, including deletion of the recombinase gene *recA* and simultaneous integration of an inducible specific sgRNA targeting the editing plasmid, combined with optimization of λRed expression and editing plasmid transformation condition, this tool could achieve 28.8 % ± 3.9 %–100 % ± 0 efficiencies for scarless editing of single targets (including DNA deletion, insertion, and promoter replacements). This tool could be used for editing of NP BGCs cloned in either a single-copy BAC plasmid pCL01 [25] or a high-copy plasmid pCAP01 [26]. We further showed that iCASRED achieved simultaneous double-target editing efficiency of 6.6 % ± 6.6 %, which could be increased to approximately 24.4 % ± 3.8 % by the replacement of Cas9 by the Cas9 nickase (nCas9, Cas9^{D10A}). For simplicity, we named this approach for editing BGCs as iCASRED (genome-integrated Cas9/λRed-based editing system). iCASRED provides a simple, convenient, and cost-effective approach for scarless editing of gene clusters, which may further facilitate the discovery of novel NPs and strain improvement for high-yield of target compounds.

2. Materials and methods

2.1. Strains, plasmids, and bacterial culture conditions

The strains, plasmids, and primers used in this study are listed in Supplementary Tables S1 and S2. *E. coli* strains were cultured at 37 °C in Luria-Bertani (LB) broth with shaking at 220 rpm or on LB agar plates. E. coli DH5α was used as the host for plasmid construction. *E. coli* Top10, DSM42 [27], EPI300, and BL21/DE3, were tested for transformation efficiency of large plasmids (harboring NP BGCs). S17-1 (methylation-rich) and ET12567/pUZ8002 (methylation-deficient) were used as the donor strains for conjugal transfer experiments between *E. coli* and *Saccharopolyspora spinosa* 301 (CGMCC No. 32535), and between *E. coli* and *Streptomyces avermitilis* MSB01, respectively. *S. avermitilis* MSB01 was a high avermectin-producing strain derived from the wild-type strain NRRL 8165 after repeated chemical and physical mutagenesis. MSB01 and its derivatives were cultured at 30 °C on MS agar medium (20 g/L soya flour, 20 g/L D-mannitol, and 20 g/L agar) for preparing spore suspensions and on MS agar medium with 10 mM $MgCl_2$ for conjugal transfer experiments. *S. spionsa* 301, which can produce spinosyn J and L, was obtained on the basis of *S. spionsa* DSM 44228 by deleting the *spnK* gene and three methylation restriction-modification (RM) system genes, including *A8926_1903/1904/1905* (encoding a type I RM system), and *A8926_1725/1726* and *A8926_2652/2653* (encoding two type II RM systems). Sas301 and its derivative strains were grown at 30 °C on 2CMC agar medium (soluble starch 10 g/L, tryptone 2 g/L, NaCl 1 g/L, $(NH_4)_2SO_4$ 2 g/L, K_2HPO_4 1 g/L, MgSO4·7H_2O 2 g/L, Casamino acid 2 g/L, $CaCO_3$ 2 g/L, agar 20 g/L and addition of trace element solution including $MnCl_2·4H_2O$ 1.55 mg/L, $ZnSO_4·7H_2O$ 1.75 mg/L, pH 7.2) for preparing spore suspensions. 2CMC with 20 mM $MgCl_2$ was employed for intergenic conjugation. If necessary, antibiotics were added at the following final concentrations, including spectinomycin (100 μg/mL), apramycin (50 μg/mL), kanamycin (50 μg/mL), chloramphenicol (25 μg/mL), and nalidixic acid (25 μg/mL).

2.2. Construction of E. coli host BL22 with chromosomal integration of Cas9/λRed expression cassettes on the basis of BL21/DE3

The chromosomal integration of Cas9/λRed expression cassettes was performed by the two-plasmid-based CRISPR-Cas9 system reported previously [24]. Briefly, the transcription cassette of sgRNA targeting the *SS9* site in the genome of BL21/DE3 was amplified using the primer pair, ins-gRNA^{SS9}-fw/gRNA-rev and pTargetF-*cat* was used as the template. The upstream and downstream arms (HAs, UHA-1166 bp and DHA-790 bp) flanking the *SS9* site were obtained by PCR using the primer pairs (ins-SS9-UHA-fw/rev and ins-SS9-DHA-fw/rev) and the BL21/DE3 genome was used as the template. Three DNA fragments were cloned into pTargetF-*cat* (pretreated with *Spe*I/*Hin*dIII) through *in vitro* recombination using 2 × Ezmax® Ultra Universal CloneMix (Tolo Biotech., China), yielding the editing plasmid pTarget-HA. The Cas9/λRed expression cassettes (8.2 kb) was amplified from the pCas plasmid using the primer pair, Cas9-λRed-fw/rev, and then cloned into the *Pme*I-linearized pTarget-HA using using 2 × Ezmax® Ultra Universal CloneMix (Tolo Biotech., China), generating the editing plasmid pTarget-*ins*-Cas9/λRed/HA. As a control, pTarget-*sg^{SS9}* with the replacement of sgRNA^{cat} in pTargetF-*cat* by *sg^{SS9}* was constructed as follows. The *sg^{SS9}* transcription cassette was amplified using gRNA^{SS9}-fw/gRNA-rev1 and pTargetF-*cat* was used as the template. The PCR product was cloned into pTargetF-*cat* pretreated with *Spe*I/*Hin*dIII using 2 × Ezmax® Ultra Universal CloneMix (Tolo Biotech., China), generating pTarget-*sg^{SS9}*. It is worth to note that compared with the primer gRNA-rev, gRNA-rev1 harbors a 31-bp short fragment homologous to the vector and a *Hin*dIII enzyme site, which could be ligated to the *Spe*I/*Hin*dIII-digested pTargetF-*cat* through *in vitro* recombination. The correctness of all the constructed editing plasmids in this study were verified by DNA sequencing.

The strain BL21/DE3-pCas was obtained by introducing pCas by electroporation. The competent cells of BL21/DE3-pCas for electroporation were prepared as follows. One colony of BL21/DE3-pCas was inoculated into 4 mL LB liquid medium. After growth overnight at 37 °C, 50 μL cultures were transferred into 50 mL LB liquid medium in 250 mL flasks. When OD_{600} of the cultures reached approximately 0.3, the inducer arabinose was added to induce λRed expression for 0.5 h at the final concentration of 10 mM. The cultures ($OD_{600} \approx 0.4$, approximately 5.0×10^8 colonies/mL) were collected and washed twice with 10 % glycerol. The editing plasmid pTarget-*ins*-Cas9/λRed/HA (100 ng) was electroporated into the competent cells of BL21/DE3-pCas using a BioRad-MicroPulser with the parameters (Bacteria, 2.5 kV, 0.2 cm cuvette), followed by incubation at 37 °C for 1.0 h. After growth on LB agar plates supplemented with kanamycin and spectinomycin overnight, the colonies with correct insertion of Cas9/λRed was confirmed by colony PCR using the primer pair (cas9J-fw/rev) combined with DNA sequencing. Plasmid curing of pTarget-*ins*-Cas9/λRed/HA and pCas was conducted as reported previously [24]. The resulting engineered strain was named as BL22.

2.3. iCASRED-based chromosomal gene deletion

iCASRED-based deletion of *bioH* and *trxA* in the genome of BL22 was

performed as follows. Here, we introduced the process for *bioH* deletion as an example. In brief, the transcription cassette of sgRNA targeting *bioH* was obtained by PCR using the primer pair, gRNA^{bioH}-fw/gRNA-rev and the pTargetF-*cat* plasmid was used as the template. The upstream and downstream arms (UHA-977 bp and DHA-682 bp) flanking *bioH* were amplified from the BL22 genome using the primer pairs (ΔbioH-up-fw/rev and ΔbioH-down-fw/rev). Three DNA fragments were cloned into pTargetF-*cat* (pretreated with *Spe*I/*Hin*dIII) simultaneously through *in vitro* recombination using 2 × Ezmax® Ultra Universal CloneMix (Tolo Biotech., China), yielding the editing plasmid pTarget-sg^{bioH}/HA. The obtained plasmid was electroporated into BL22 competent cells, which were prepared as that of BL21/DE3-pCas described above. 10 colonies were randomly selected for colony PCR analysis using the verification primer pair, *ΔbioH*-J-fw/rev. The colonies with correct *bioH* deletion were further verified by PCR product sequencing.

The BL23 host with the deletion of *recA* and simultaneous insertion of sg^T transcription module (including the $lacI^q$ expression cassette and the P_{trc}-driven transcription cassette of sgRNA targeting the spectinomycin resistance gene spe^R of the editing plasmid, 1696 bp) on the basis of BL22 was also constructed using iCASRED-based editing. Briefly, the sgRNA targeting *recA* was obtained by PCR using the primer pair, gRNA^{recA}-fw/gRNA-rev and pTargetF-*cat* was used as the template. The upstream and downstream arms (UHA-1166 and DHA-790 bp) flanking *recA* were obtained by PCR using two respective primer pairs (ΔrecA-up-fw/rev and ΔrecA-down-fw/rev) and the BL22 genome was used as the template. The sg^T transcription module was amplified from pCas using the primers sg^T-fw/rev. The four fragments (in the order of sgRNA^{recA}, UHA, sg^T, and DHA) were cloned into pTargetF-*cat* (pretreated with *Spe*I/*Hin*dIII) through *in vitro* recombination using 2 × Ezmax® Ultra Universal CloneMix (Tolo Biotech., China), resulting in the editing plasmid pTarget-Δ*recA*:sg^T/HA. Similarly, the obtained plasmid (100 ng) was electroporated into BL22 competent cells induced by 10 mM arabinose. Colonies with correct *recA* deletion and sg^T insertion were verified by colony PCR using the verification primer pair (ΔrecA-J-fw/rev) combined with DNA sequencing.

The BL24 host with the replacement of the *Cas9* gene with *nCas9* was constructed similarly as above on the basis of BL23. The constructed plasmids and primers used for the construction of the editing plasmid as well as for mutant verification are listed in Supplementary Tables S1 and S2.

For the curing of editing plasmids, the edited colonies were inoculated into 4 mL of LB liquid medium with 1.0 mM IPTG (isopropyl-β-D-thiogalactopyranoside), followed by incubated at 37 °C for 8–16 h. Cultures were diluted and spread onto LB agar plates. Colonies with the removal of editing plasmids could grow on LB plates without spectinomycin, but not on LB plates with spectinomycin.

2.4. iCASRED-based NP BGC editing

The editing plasmids for iCASRED-based single-target editing of NP BGC cloned in either pCL01 or pCAP01 were constructed as follows. Here, we used the construction of the editing plasmid for *milF* insertion into pCL01-*omil* as an example. Briefly, the transcription cassette of sgRNA targeting the region between *SBI_00730* and *SBI_00732* was obtained by PCR using the primer pair gRNA^{milF}-fw/gRNA-rev and pTargetF-*cat* was used as the template. The DNA fragment containing two HAs (UHA-644 bp and DHA-554 bp) and the *milF* gene was obtained by PCR from the *Streptomyces milbemycinicus* SIPI-054 genome using the primer pair, milF-fw/rev. The above two PCR products were cloned into pTargetF-*cat* (pretreated with *Spe*I/*Hin*dIII) simultaneously through *in vitro* recombination using 2 × Ezmax® Ultra Universal CloneMix (Tolo Biotech., China), yielding the editing plasmid pTarget-$sg^{ins\text{-}milF}$/HA. As controls, the recombinant plasmids with the cloning of only sgRNA transcription cassette, such as pTarget-$sg^{ins\text{-}milF}$, pTarget-sg^{milE}, and pTarget-$sg^{milR\text{-}kasOp*}$, were constructed similarly as that of pTarget-sg^{SS9} by replacing sgRNA^{cat} in pTargetF-*cat* with the corresponding sgRNA transcription cassettte through *in vitro* recombination.

The obtained plasmids were electroporated into BL22 or BL23 competent cells, which were prepared as that of BL21/DE3-pCas described above. After each transformation experiment, 15 colonies were randomly selected for colony PCR analysis using the verification primer pairs (e.g. milF-J-fw/rev). Colonies with correct gene editing were further verified by PCR product sequencing.

The editing plasmid for iCASRED or inCASRED-based double-target editing of pCL01-*omil* was constructed as follows. Here, we take the construction of iCASRED-based double-editing plasmid for *milE* deletion and simultaneous *milR* promoter replacement as an example. In brief, the DNA fragment $sg^{milR\text{-}kasOp*}$/HA containing $sg^{milR\text{-}kasOp*}$ and two corresponding HAs were amplified from pTarget-$sg^{milR\text{-}kasOp*}$/HA using the primers of gRNA$^{milR\text{-}kasOp*}$-fw/milR-kasOp*-down-rev. The obtained product was cloned into *Hin*dIII-linearized pTarget-sg^{milE}/HA using 2 × Ezmax® Ultra Universal CloneMix (Tolo Biotech., China), to yield the double-target editing plasmid pTarget-sg^{milE}/HA-$sg^{milR\text{-}kasOp*}$/HA.

For optimization of iCASRED-based BGC editing, three different parameters, including arabinose concentrations for λRed expression, the duration for arabinose induction, and the recovery time after editing plasmid transformation, were explored. The editing efficiency of *milE* deletion was tested.

I. *Arabinose concentrations for λRed expression.* Colonies of the recombinant BL23 harboring pCL01-*omil* were inoculated into 4 mL LB liquid medium. After growth overnight at 37 °C, 50 μL cultures were transferred to 50 mL LB liquid medium in 250 mL flasks. When OD_{600} reached approximately 0.3, arabinose was added to induce λRed expression for 0.5 h at different final concentrations (0.1, 0.5, 1.0, 2.5, 10 mM). The cultures ($OD_{600} \approx 0.4$, approximately 5.0×10^8 colonies/mL) were collected and washed twice with 10 % glycerol. The editing plasmids (100 ng each) were electroporated into the competent cells using a BioRad-MicroPulser with the parameters (Bacteria, 2.5 kV, 0.2 cm cuvette), followed by incubation for 1.0 h.

II. *The duration for arabinose induction.* After growth overnight of the recombinant BL23 harboring pCL01-*omil* in 4-mL LB liquid medium at 37 °C, 50 μL cultures were transferred to 50 mL LB liquid medium in 250 mL flasks, followed by the addition of arabinose (the final concentration of 10 mM) at four different time points (0, 2.0, 3.0, 3.5, and 4.0 h) to induce λRed expression. The corresponding duration time of arabinose induction was 4.0, 2.0, 1.0, 0.5, and 0 h. The editing plasmid (100 ng each) were electroporated into the competent cells followed by incubation for 1.0 h.

III. *The recovery time after editing plasmid transformation.* The editing plasmid pTarget-sg^{milE}/HA (100 ng) were electroporated into the competent cells of BL23/pCL01-*omil* induced by 10 mM arabinose for 2.0 h, followed by incubation for 0, 1.0, 2.0, and 4.0 h.

After each transformation experiment, the transformation mixtures were spread on LB agar plates supplemented with apramycin and spectinomycin overnight and 15 colonies were randomly selected for colony PCR analysis using the verification primer pairs. The colonies with correct *milE* deletion were further confirmed by DNA sequencing.

It is worth to note that, for the editing of BGCs cloned in pCAP01, the transformation mixtures were spread on LB agar plates with kanamycin and spectinomycin, and other steps are the same as those for the editing of BGCs cloned in pCL01 as described above.

2.5. TAR-based cloning of NP BACs

The spinosyns BGC (*spi*) were cloned using TAR cloning method in yeast as described previously [26] and pCL01, which is a BAC plasmid derived from the copy-control plasmid pCC1BAC [25], was used as the cloning vector. The epirubisin BGC (*epi*) was cloned in a high-copy

plasmid pCAP01 using the same TAR method. Here, the TAR-based cloning of *spi* BGC was described as an example and the detailed information was presented in the Supplementary materials.

2.6. Construction of the S. avermitilis host strain with the deletion of the avermectin BGC

The deletion of the 85.1 kb-long DNA fragment (from *SAVERM_RS05150* to *SAVERM_RS05265*) containing the avermectin BGC (*ave*, 80.0 kb) in the genome of *S. avermitilis* MSB01 was performed using CRISPR/Cas9-based method reported previously [28]. Briefly, the transcription cassette of sgRNA targeting *SAVERM_RS05260* was amplified from pKCCas9 using the primer pair, gRNA$^{\Delta ave}$-N20-fw/rev. Two HAs (UHA- 2093 bp and DHA-1891 bp) flanking the *ave* gene cluster were obtained by PCR using Δave-up-fw/rev and Δave-down-fw/rev, respectively and the MSB01 genome was used as the template. Notably, to introduce an artificial φC31-integrase recognition *attB* site into the host genome, the primer Δave-down-fw was designed to harbor a synthesized φC31 *attB* sequence at the 5′-terminus. Then, the above three PCR products were ligated together by PCR using the primers gRNA$^{\Delta ave}$-N20-fw/Δave-down-rev (harboring two respective 25-bp overlapping extensions homologous to the terminal regions of *Spe*I/*Hin*dIII-linearized pKCCas9). The products were ligated to *Spe*I/*Hin*dIII linearized pKCCas9 through *in vitro* recombination using 2 × Ezmax® Ultra Universal CloneMix (Tolo Biotech., China), resulting in the editing plasmid pKCCas9-*sg^{ave}*/HA.

The obtained plasmid was introduced into MSB01 by intergenic conjugation. The exconjugants with the correct deletion of the *ave* BGC and simultaneous insertion of an artificial φC31-*attB* site were verified by colony PCR using the primer pair, Δave-J-out-fw/rev targeting outside of two HAs, followed by PCR product sequencing. As a control, the primer pair Δave-J-in-fw/rev was designed to amplify DNA fragment in the *ave* BGC. If the *ave* BGC was deleted, we could not obtain the PCR products using Δave-J-in-fw/rev. For curing the editing plasmid, positive colonies were passaged on MS agar for three times at 37 °C. The obtained mutant strain was named as Δ*ave*.

2.7. Fermentation of the engineered Streptomyces strains and HPLC analysis of milbemycins or 5-oxomilbemycins production

Three recombinant plasmids, including pCL01-*omil*, pCL01-*omil*:*milF*, and pCL01-*omil*:*milF-milR-kasOp**, were introduced into Δ*ave* by intergenic conjugation. Colony PCR was used to identify the positive exconjugants with the integration of the target BGCs using the primer pairs, attB-L-fw/attP-R-rev, attP-L-fw/attB-R-rev, respectively, followed by PCR product sequencing. We obtained three engineered strains, namely, Δ*ave*/pCL01-*omil*, Δ*ave*/pCL01-*omil*:*milF*, and Δ*ave*/pCL01-*omil*:*milF-milR-kasOp**.

The colonies of the host *S. avermitilis* MSB01 and its derivatives, including Δ*ave*/pCL01-*omil*, Δ*ave*/pCL01-*omil*:*milF,* and Δ*ave*/pCL01 and Δ*ave*/pCL01-*omil*:*milF/milR-kasOp**, were streaked on MS agar plates and grown 30°C for 6 days. The agar cultures (approximately 1 cm^2) were inoculated into 25 mL seed culture medium/250-mL flasks (corn starch 10 g/L, soybean meal 10 g/L, glucose 5 g/L, cottonseed cake powder 20 g/L, pH = 7.2 ± 0.2), followed by incubation at 28°C, 220 rpm for 40–60 h. Then, 3 mL of seed cultures were transferred into 30 mL fermentation medium (250-mL flasks) (corn starch 50 g/L, soybean meal 10 g/L, cottonseed cake powder 10 g/L, α-amylase 0.1 g/L, NaCl 5 g/L, $CaCO_3$ 7 g/L, pH 7.1 ± 0.1) and grown at 28°C, 220 rpm for 10 days.

500 μL of fermentation cultures were collected and extracted with 1.5 mL of anhydrous ethanol, followed by ultrasound for 30 min. After centrifugation at 12,000 *g* for 5 min, the supernatants were analyzed by HPLC (high-performance liquid chromatography) using a reversed-phase column (Hypersil-C18, 4.6 mm × 150 mm, 5 μm). The mobile phase is a mixture of acetonitrile/water (73:27) with a flow rate of 1.2 mL/min. Milbemycins and 5-oxo-milbemycins were detected at a wavelength of 240 nm. The retention time of milbemycin A3/A4 (the main components of milbemycins) are 10.2 min and 12.7 min, while the retention times of 5-oxomilbemycin A3/A4 (the main components of 5-oxo-milbemycins) are 11.8 min and 15.3 min. *S. avermitilis* fermentation was performed with three independent biological replicates. Error bars indicate the standard deviation of three independent experiments.

2.8. Fermentation of the engineered S. spinosa strains and HPLC analysis of spinosyns production

Three recombinant plasmids, including pCL01*int32-spi*, pCL01*int32-spiΔspnK*, and pCL01*int32-spiΔspnK/L16-kasOp**, were introduced into *S. spinosa* 301 by conjugal transfer, generating the engineered strains, including 301/pCL01*int32-spi*, 301/pCL01*int32-spiΔspnK*, and 301/pCL01*int32-spiΔspnK/L16-kasOp**.

For *S. spinosa* fermentation, *S. spinosa* 301 agar cultures (1 cm^2) were inoculated into seed cultures in a 250 mL Erlenmeyer flask with 30 mL of seed medium (beef extract 1 g/L, yeast extract 5 g/L, tryptone 5 g/L, glucose 5 g/L, $MgSO_4$ 2 g/L, pH 7.4), followed by incubation for 3–4 days at 28 °C. Then, 3 mL of seed cultures was transferred into a 250 mL Erlenmeyer flask containing 30-mL fermentation medium (yeast extract 6 g/L, corn steep powder 10 g/L, cake powder 15 g/L, cottonseed meal 10 g/L, glucose 6 g/L, $FeSO_4$ 0.05 g/L, soybean oil 6 g/L, $CaCO_3$ 5 g/L, pH 7.4). Fermentation was conducted at 28 °C and 220 rpm. Fermentation experiments were performed in triplicates. After 10 days, 200 μL fermentation cultures were collected and mixed with 800 μL ethanol, followed by sonication 30 min at room temperature and centrifugation at 10,000 rpm for 10 min, respectively. The supernatants were subjected to HPLC analysis (ZORBAX Ecllipe XDB-C18, 4.6 × 100 mm, 5 μm) at the wavelength of 246 nm. Methanol/acetonitrile/2 % ammonium acetate (v/v/v = 45:45:10) was used as a mobile phase with the flow rate of 1.0 mL/min. The standards of spinosyn A/D and J/L were used for quality and quantitative analysis.

3. Results

3.1. Design of iCASRED-based BGC editing system in E. coli

Here, the two-plasmid-based CRISPR-Cas9 genome editing tool developed previously in *E. coli* [24] was extended for *in vivo* editing of the NP BGCs cloned in either a single-copy BAC plasmid or a high-copy plasmid (e.g. pCAP01). To achieve this goal, we engineered the *E. coli* host from the following three main steps. Firstly, the Cas9/λRed expression cassettes from the CRISPR-Cas9 genome editing tool [24], in which *cas9* is driven by its native promoter and the λRed genes (*exo*, *bet*, and *gam*) are under the control of the arabinose-inducible promoter P_{araB}, was integrated into the genome to simplify the editing system. Secondly, the host *recA* gene involved in the repair of double-stranded breaks (DSBs) was inactivated to increase iCASRED-based editing efficiency. Thirdly, a Trc promoter-driven transcription cassette of sgRNA targeting the editing plasmid was pre-inserted into the genome to facilitate plasmid curing by IPTG induction (Fig. 1).

In the iCASRED system, an all-in-one editing plasmid containing both the sgRNA(s) targeting the NP BGC and two homology arms (HAs) was constructed and introduced into the competent *E. coli* cells (induced by arabinose for λRed expression) containing the recombinant plasmid with the cloning of the NP BGC (BAC-BGC). DSBs generated by Cas9/sgRNA could be repaired by the λRed system using the provided HAs in the editing plasmid [24]. Once positive colonies with target edited BGCs were obtained, the curing of editing plasmids could be achieved by IPTG induction, enabling a new round of BGC editing (Fig. 1).

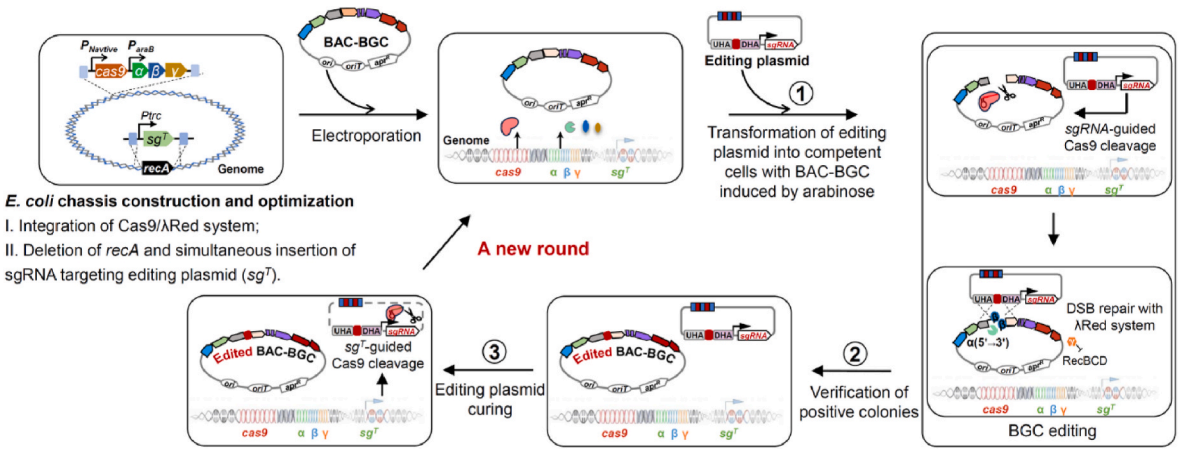

Fig. 1. Overview of the iCASRED-based BGC editing system in *E. coli*.

3.2. BL21/DE3 used as the host for iCASRED-mediated DNA editing due to its higher DNA transformation efficiency of large-sized plasmids

To facilitate gene cluster editing in *E.coli*, a high transformation efficiency of large-sized plasmids is required. Here, four *E. coli* strains, including BL21/DE3, Top10, EPI300, and MDS42 [27], were tested for the transformation of two large-sized plasmids, including pCL01-*omil* (84.7 kb) [25] and pCAP01-*epi* (53.3 kb) with the 72.0-kb 5-oxo--milbemycin BGC and 44.2 kb epirubicin BGC cloned in the BAC vector pCL01 and the high-copy plasmid pCAP01, respectively. pCAP01-*epi* was constructed by TAR cloning tool in yeast (data not shown). We found that among the tested strains, BL21/DE3 exhibited the highest DNA transformation efficiency. Therefore, in this study, it was used as the host for iCASRED-mediated BGC editing (Fig. 2A).

3.3. Chromosomal integration of Cas9/λRed into BL21/DE3 retained its high-efficiency genome editing ability

To construct the *E. coli* chassis for iCASRED-based BGC editing, as the first step, the Cas9/λRed expression cassettes were integrated into BL21/DE3 genome using the two-plasmid-based CRISPR-Cas9 system [24]. The safe site 9 (*SS9*) of BL21/DE3, which was identified as a genomic site with a high integration efficiency and gene expression level without affecting cell growth [29], was selected as the integration site (Supplementary Fig. S1A). The editing plasmid pTarget-*ins*-Cas9/λRed/HA, which contains the sgRNA targeting the *SS9* site and the Cas9/λRed expression cassettes flanked by two HAs, was constructed (Supplementary Fig. S1B). Introduction of the editing plasmid into the competent cells of BL21/DE3-pCas induced by arabinose resulted in successful insertion of Cas9/λRed verified by colony PCR (Supplementary Fig. S1C) and DNA sequencing (data not shown). After curing both pTarget-*ins*-Cas9/λRed-HA and pCas using the method described previously [24], we obtained the engineered strain BL22.

To check whether the iCASRED system in BL22 retained its genome editing ability, two genes, namely, *bioH* (encoding a methylesterase involved in biotin synthesis) [30] and *trxA* (encoding a thioredoxin) [31], were selected as the deletion targets. Two editing plasmids, including pTarget-sg^{trxA}/HA and pTarget-sg^{bioH}/HA, were generated. As controls, two recombinant plasmids without HAs, namely, pTarget-sg^{trxA} and pTarget-sg^{bioH}, were constructed as well. We showed that introduction of two control plasmids (pTarget-sg^{trxA} and pTarget-sg^{bioH}) led to the formation of a small number of colonies, indicating the integrated expression of Cas9 functioned well under the guidance of the provided specific sgRNA. These two editing plasmids yielded more colonies than their corresponding controls (Fig. 2B), which should be due to λRed-based DSB repair using the provided HA. Further colony PCR and DNA sequencing revealed that iCASRED could achieve 100 % and 95 % editing efficiency for the deletion of *trxA* and *bioH*, respectively (Fig. 2C and Supplementary Fig. S2), clearly indicating that iCASRED maintained its activity well and enabled high-efficiency genome editing in *E. coli* BL22. Here, it is worth to note that the curing of the editing plasmids harboring the *pMB1* replicon is time-consuming, which required blind passages for at least five times in liquid LB medium (data not shown).

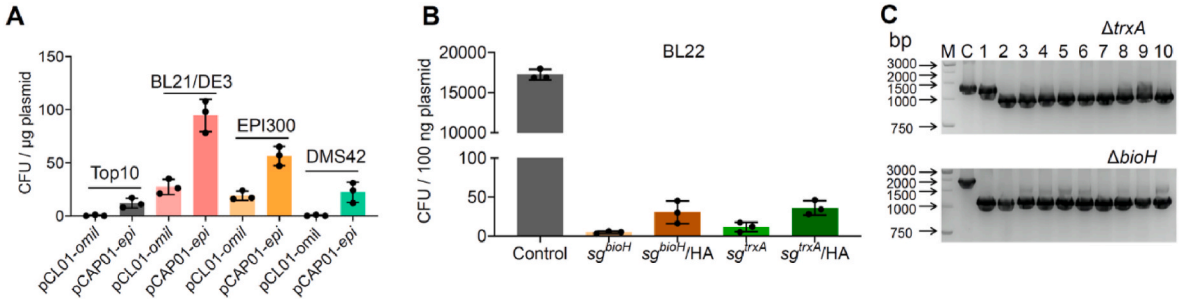

Fig. 2. Integrated expression of Cas9/λRed in BL21/DE3 maintains its high-efficiency genome editing ability. (**A**) Transformation efficiencies of two large-sized plasmids, pCL01-*omil* and pCAP01-*epi*. Four *E. coli* strains as presented were tested. CFU: colony formation units; 1 μg of each plasmid was used for each transformation experiment. The error bars represent the standard deviations of the transformation efficiencies from three independent experiments. (**B**) The efficiencies of the transformation of editing plasmids into *E. coli* BL22. The efficiencies were indicated by CFU/100 ng plasmids. Two editing plasmids, including pTarget-sg^{bioH}/HA (sg^{bioH}/HA) and pTarget-sg^{trxA}/HA (sg^{trxA}/HA), were tested. Two plasmids with sgRNAs only, including pTarget-sg^{bioH} (sg^{bioH}) and pTarget-sg^{trxA} (sg^{trxA}), were used as controls. Control: pTargetF-*no*. The error bars represent the standard deviations of the transformation efficiencies from three independent experiments. (**C**) Colony PCR analysis of iCASRED-based gene deletion in the genome of BL22. Two genes, including *bioH* and *trxA*, were tested. One presentative colony PCR result was presented.

3.4. iCASRED-based engineering of NP BGC cloned in a BAC plasmid

To determine whether the iCASRED system could be employed to engineer NP BGCs, herein, the editing of pCL01-*omil* was used as an example, and three different editing types, including deletion of *milE*, insertion of *milF*, and replacement of the native promoter of *milR* by the strong constitutive promoter *kasOp** [32], were tested (Fig. 3A). Three editing plasmids, namely, pTarget-sg^{milE}/HA, pTarget-$sg^{ins\text{-}milF}$/HA, and pTarget-$sg^{milR\text{-}kasOp*}$/HA, which contain both the respective sgRNA and two HAs, and three control plasmids, including pTarget-sg^{milE}, pTarget-$sg^{ins\text{-}milF}$, and pTarget-$sg^{milR\text{-}kasOp*}$ with only the specific targeting sgRNAs, were constructed. They were individually electroporated into the competent cells of BL22/pCL01-*omil* induced by arabinose for λRed expression. The pTargetF-*no* plasmid without the 20-bp guide sequence of sgRNA was used as a control. We showed that, interestingly, introduction of these three control plasmids led to the formation of a large number of colonies (Fig. 3B), which are much more than those obtained for pTarget-sg^{trxA} and pTarget-sg^{bioH} targeting the genome. Sequencing of the PCR products using primers annealing outside the HAs revealed that they are all unedited strains (data not shown). We reasoned that this phenomenon might be ascribed to the lower ability of Cas9-based BAC DNA cleavage than that of *E. coli* genome, which should be associated with the faster replication speed of the BAC plasmid. Colony PCR analysis combined with DNA sequencing showed that iCASRED achieved approximately 42.2 % ± 6.7 %, 11.1 % ± 3.9 %, and 24.4 % ± 3.8 % editing efficiency for *milE* deletion, *milF* insertion, and promoter replacement of *milR*, respectively (Fig. 3C and Supplementary Fig. S3). The results clearly indicated that iCASRED in BL22 could be employed for BGC editing. Similarly, curing of the editing plasmids required blind passages for at least five times in liquid LB medium (data not shown).

3.5. Deletion of recA significantly increased the efficiency of iCASRED-mediated BGC editing

It was reported that the deletion of *recA* resulted in significantly increased Cas9/λRed-based genome engineering efficiency [33]. Thus, to determine whether the iCASRED-based BGC editing ability could be enhanced similarly by *recA* deletion, we deleted the *recA* gene on the basis of BL22. In addition, to facilitate editing plasmid curing, we inserted the control module sg^T, which includes the $lacI^q$ expression cassette and the inducible promoter P_{trc}-driven transcription cassette of sgRNA targeting the spectinomycin resistance gene (spe^R) of the editing plasmid, when deleting the *recA* gene (Fig. 4A). The editing plasmid pTarget-Δ*recA*:sg^T/HA was constructed and introduced into BL22 competent cells induced by arabinose. Colony PCR analysis showed that iCASRED-based genome editing tool achieved approximately 80 % efficiency of *recA* deletion with simultaneous insertion of the sg^T module (Supplementary Fig. S4A), which was further confirmed by DNA sequencing (data not shown). We showed that compared with the difficulty for editing plasmid curing in BL22, the editing plasmid pTarget-Δ*recA*:sg^T/HA could be cured at 100 % efficiency in the engineered strain (named as BL23) after induction by 1 mM IPTG (Supplementary Fig. S4B). However, as a control, without IPTG induction, the editing plasmid could also be cured at an efficiency of 80 %, suggesting the leaked transcription of sg^T. iCASRED-based genome editing efficiency in BL23 was measured and *bioH* was used as the deletion target. We showed that iCASRED in BL23 achieved 100 % efficiency of *bioH* deletion as that in BL22 (Supplementary Fig. S4C), clearly indicating that *recA* deletion and simultaneous sg^T insertion had no effect on genome editing ability of iCASRED.

Then, the efficiencies of iCASRED-mediated pCL-*omil* editing, including *milE* deletion, *milF* insertion, and replacement of the native promoter of *milR* by *kasOp**, were compared between BL22 and BL23.

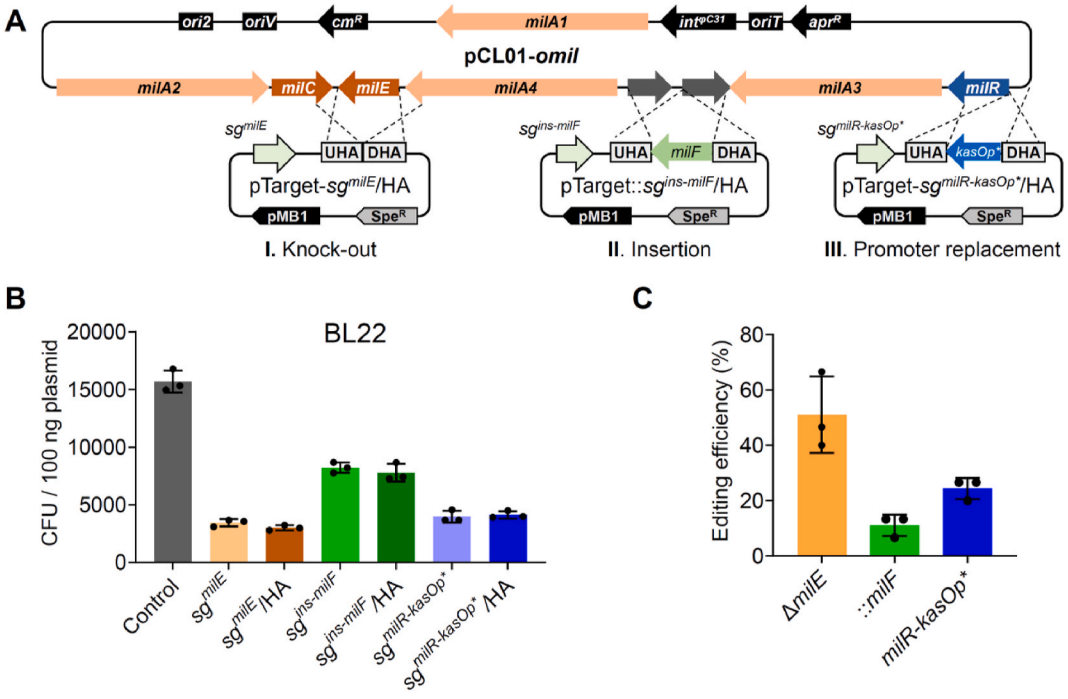

Fig. 3. The efficiencies of iCASRED-based 5-oxo-milbemycin BGC editing in *E. coli* BL22. (**A**) Schematic map of iCASRED-based BGC editing, including gene knock-out, insertion, and promoter replacement. The BAC-derived pCL01-*omil* with the cloning of 72.0 kb 5-oxo-milbemycin BGC was tested. (**B**) The efficiencies of the transformation of editing plasmids into BL22. The efficiencies were indicated by CFU/100 ng plasmids. Three editing plasmids, including pTarget-sg^{milE}/HA (sg^{milE}/HA), pTarget-$sg^{ins\text{-}milF}$/HA ($sg^{ins\text{-}milF}$/HA), and pTarget-$sg^{milR\text{-}kasOp*}$/HA ($sg^{milR\text{-}kasOp*}$/HA), were tested. Three plasmids with sgRNAs only, including pTarget-sg^{milE} (sg^{milE}), pTarget-$sg^{ins\text{-}milF}$ ($sg^{ins\text{-}milF}$), and pTarget-$sg^{milR\text{-}kasOp*}$ ($sg^{milR\text{-}kasOp*}$), were used as controls. Control: pTargtF-*no*. The error bars represent the standard deviations of the transformation efficiencies from three independent experiments. (**C**) Editing efficiencies of iCASRED-based *milE* deletion, *milF* insertion and *milR* promoter replacement in BL22. The error bars represent the standard deviations of the editing efficiencies from three independent experiments.

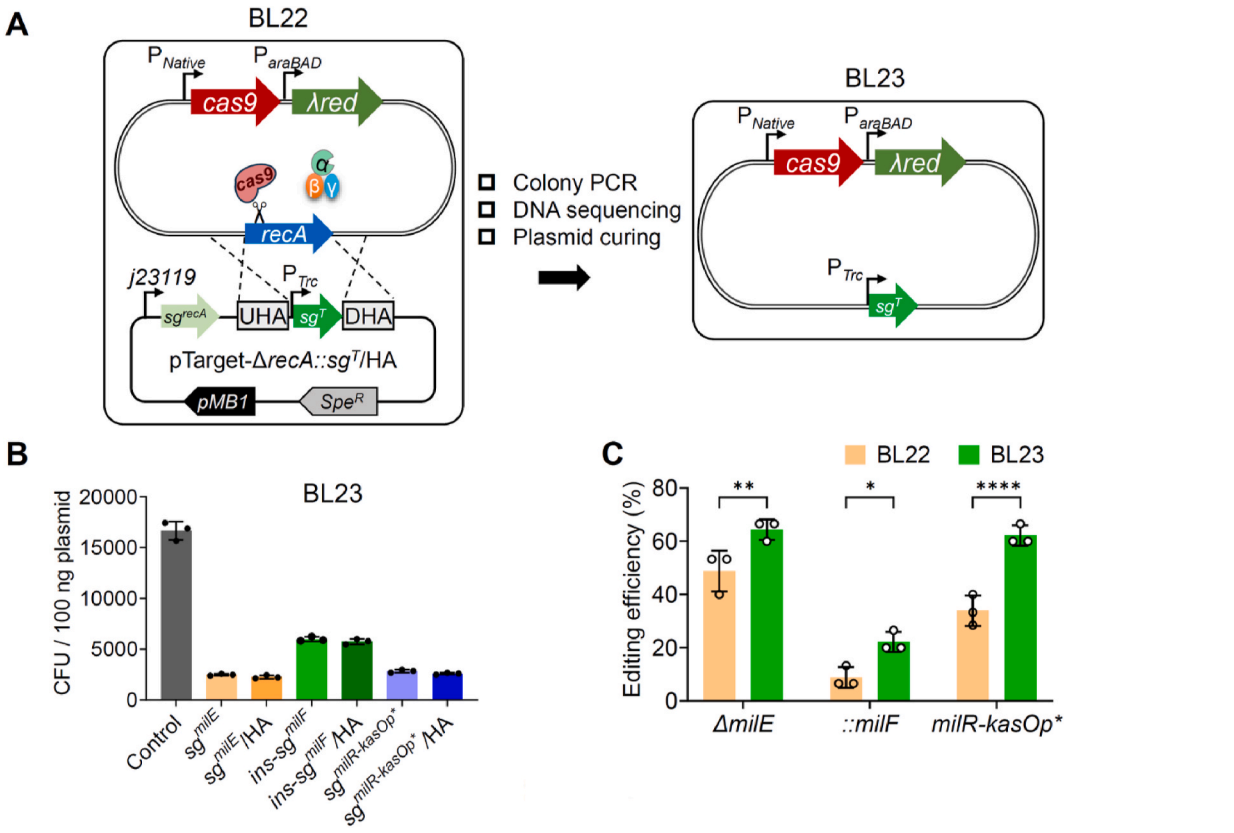

Fig. 4. Chassis optimization for iCASRED-mediated BGC editing via *recA* deletion combined by integration of the sg^T module targeting the editing plasmid. (**A**) Schematic map of chassis optimization for iCASRED-mediated BGC editing. On the basis of BL22, the host *recA* gene was deleted and simultaneously the sg^T module (includes the $lacI^q$ expression cassette and the inducible promoter P_{trc}-driven transcription cassette of sgRNA targeting the spectinomycin resistance gene (spe^R) of the editing plasmid) was inserted using iCASRED-based genome editing tool, which resulted in the construction of BL23 chassis. (**B**) Efficiencies of the transformation of editing plasmids into *E. coli* BL23. The efficiencies were indicated by CFU/100 ng plasmids. Three editing plasmids, including pTarget-sg^{milE}/HA (sg^{milE}/HA), pTarget-$sg^{ins\text{-}milF}$/HA ($sg^{ins\text{-}milF}$/HA), and pTarget-$sg^{milR\text{-}kasOp*}$/HA ($sg^{milR\text{-}kasOp*}$/HA), were tested. Three plasmids with sgRNAs only, including pTarget-sg^{milE} (sg^{milE}), pTarget-$sg^{ins\text{-}milF}$ ($sg^{ins\text{-}milF}$), and pTarget-$sg^{milR\text{-}kasOp*}$ ($sg^{milR\text{-}kasOp*}$), were used as controls. Control: pTargtF-*no*. The error bars represent the standard deviations of the transformation efficiencies from three independent experiments. (**C**) Comparison of editing efficiencies of iCASRED-based *milE* deletion, *milF* insertion and *milR* promoter replacement in BL22 and BL23 chassis. The error bars represent the standard deviations of the editing efficiencies from three independent experiments. *P < 0.05, **P < 0.01, ****P < 0.0001, calculated by one-way ANOVA + Tukey's multiple comparison test.

We showed that individual introduction of these three editing plasmids and the corresponding control plasmids into BL23/pCL01-*omil* led to the formation of significantly reduced exconjugant numbers as compared with those of BL22/pCL01-*omil* (Fig. 4B), which should be ascribed to the leaked expression of sg^T. Colony PCR combined with DNA sequencing revealed that the editing efficiencies of these three targets in BL23 were approximately 64.4 % ± 3.9 % for *milE* deletion, 22.2 % ± 3.8 % for *milF* insertion, and 62.2 % ± 3.8 % for promoter replacement of *milR*, which were significantly higher than those in BL22 (approximately 48.9 % ± 7.7 %, 8.9 % ± 3.9 % and 33.3 % ± 5.8 %, respectively) (Fig. 4C and Supplementary Fig. S5). The editing plasmids pTarget-sg^{milE}/HA, pTarget-$sg^{ins\text{-}milF}$/HA, and pTarget-$sg^{milR\text{-}kasOp*}$/HA were easily cured at 100 % efficiency in BL23/pCL01-*omil* after IPTG induction (data not shown). The above results clearly showed that BL23 was a better chassis for iCASRED-based gene cluster editing than BL22.

3.6. Parameter optimization of iCASRED editing tool further increased BGC editing efficiency

To further enhance iCASRED-based gene cluster editing efficiency in BL23, three main parameters of the editing tool, including arabinose concentrations for λRed expression, the duration time for arabinose induction, and the recovery duration after editing plasmid transformation were examined. iCASRED-based *milE* deletion was tested as an example. The experimental conditions before optimization were as those reported for genome editing tool in *E. coli*: arabinose concentration, 10 mM; induction time, 0.5 h; recovery time, 1 h [24]. We showed that iCASRED-based *milE* deletion achieved the optimum editing efficiency when arabinose concentrations were higher than 2.5 mM (Fig. 5A and Supplementary Fig. S6). Under arabinose induction with 10 mM concentration, *milE* deletion efficiency could be significantly increased when the induced duration was extended from 0.5 h to 1.0–2.0 h (Fig. 5B and Supplementary Fig. S7). However, further increasing the induced duration would eventually reduce the editing efficiency. Based on λRed expression induced by 10 mM arabinose for 1.0 h, we found that the highest editing efficiency was achieved by directly coating agar plate immediately after electroporation of editing plasmid into the competent cells (Fig. 5C and Supplementary Fig. S8).

We also checked whether shorter HA lengths in the editing plasmid can still work well. Three shorter HA lengths, including 50, 100, and 200 bp, were tested. The results showed that, under the above optimal parameters, 500 bp-length of each HA in the editing plasmid led to the optimum *milE* deletion efficiency (an average of 93.3 % ± 5.8 % efficiency), shorter HA lengths significantly reduced editing efficiency (Fig. 5D and Supplementary Fig. S9).

Finally, the editing efficiencies for the replacement of the native promoter of *milR* by *kasOp** and *milF* insertion were determined using the optimized parameters. We found that the efficiencies of these two types of editing could be further increased from 62.2 % ± 3.8 % to 97.8 % ± 3.9 % and from 22.2 % ± 3.8 % to 46.6 % ± 6.6 %, respectively

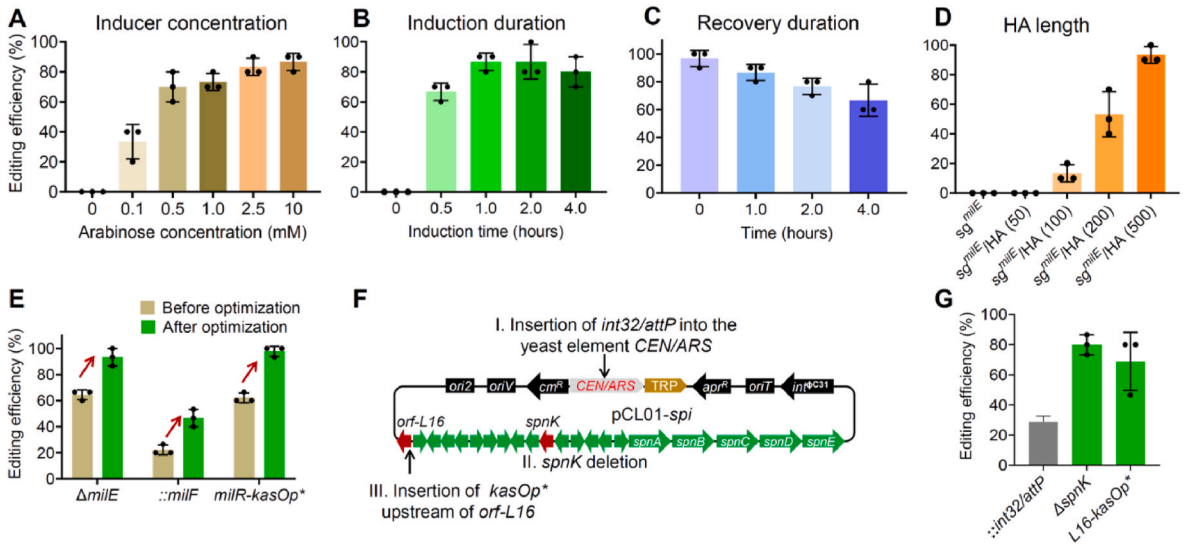

Fig. 5. Parameter optimization of iCASRED-based editing tool further increased NP BGC editing efficiency. (**A**) Efficiencies of *milE* deletion after induction for λRed expression with different arabinose concentrations as indicated. Other parameters: induction duration 0.5 h, recovery duration 1.0 h. (**B**) Efficiencies of *milE* deletion after induction of 10 mM arabinose for different time durations as indicated. Recovery duration was 1.0 h. (**C**) Efficiencies of *milE* deletion using different recovery durations after editing plasmid transformation as indicated. Other parameters: arabinose concentration 10 mM, induction duration 1.0 h. (**D**) Efficiencies of *milE* deletion using editing plasmids with different HA lengths as indicated. Other parameters: arabinose concentration 10 mM, induction duration 1.0 h, and recovery duration 0 h. (**E**) Comparison of the efficiencies of *milE* deletion, *milF* insertion, and *milR* promoter replacement before and after parameter optimization. The optimal parameters were arabinose concentration 10 mM, induction duration 1.0 h, recovery duration 0 h and HA length 500 bp. (**F**) Schematic diagram of the BAC recombinant plasmid pCL01-*spi* with the cloning of the spinosyns BGCs (76.2 kb). Three types of editing to be conducted are as presented. (**G**) Efficiencies of iCASRED-based DNA insertion (*int32/attP*), gene deletion (*spnK*) and promoter insertion (insertion of *kasOp** upstream of *orf-L16*) in pCL01-*spi*. The error bars represent the standard deviations of the editing efficiencies from three independent experiments.

(Fig. 5E and Supplementary Fig. S10).

Using the optimized conditions, a large BAC-based recombinant plasmid (pCL01-*spi*) with a 76.2 kb spinosyn A/D BGC, which was constructed using TAR cloning (data not shown) [26], was further tested for iCASRED-based editing. In pCL01-*spi*, the φC31 integrase could not mediate efficient site-specific integration in *S. spinosa* (data not shown). A previous report showed that the integrase gene (*int32*) with its native promoter and *attP* site of pCM32 enables high-efficiency site-specific integration [34]. Here, iCASRED-based editing was conducted to insert *int32/attP* (1921 bp) into the yeast element (*CEN6/ARS4*), which has been identified to be toxic to *Streptomyces* strains [25]. In addition, two genes in spinosyn A/D BGC, including *spnK* and *orf-L16*, were selected for gene deletion (*spnK*) and promoter insertion (insertion of *kasOp** upstream of *orf-L16*) (Fig. 5F). Three editing plasmids were constructed and introduced into the competent cells of BL23/pCL01-*spi* (Supplementary Fig. S11A). Colony PCR combined DNA sequencing showed that iCASRED in BL23 achieved the efficiencies of 28.8 % ± 3.9 %, 80.0 % ± 6.7 %, and 68.9 % ± 19.3 % for the insertion of *int32/attP*, *spnK* deletion, and insertion of *kasOp** upstream of *orf-L16* in pCL01-*spi*, respectively (Fig. 5G and Supplementary Figs. S11B–E). The results revealed that, the optimized iCASRED-based editing tool could achieve high-efficiency BGC editing in the chassis BL23, including DNA deletions, insertions and promoter replacements.

3.7. iCASRED-based editing of BGCs cloned in the high-copy plasmid pCAP01

As we know, a large number of NP BGCs (normally smaller than 50 kb) are cloned by cosmid/fosmid vector-based library construction [35–37] or by TAR cloning in yeast using pCAP01 [18]. These vectors are high-copy plasmids with pUC or pBR322 *ori*. Here, we further assessed whether iCASRED in BL23 could be used to edit NP BGCs cloned in high-copy plasmids. pCAP01-*epi* with the cloning of the epirubicin BGC (*epi*, 44.2 kb) in pCAP01 (pUC *ori*) was tested as an example.

In pCAP01-*epi*, two types of editing, including insertion of *kasOp** upstream of *doxA* and *dnrO* deletion, were conducted (Supplementary Fig. S12A). Two editing plasmids were constructed and introduced into the competent cells of BL23/pCAP01-*epi* (Supplementary Fig. S12B). Colony PCR showed that iCASRED in BL23 achieved 86.7 % ± 3.8 % and 100 % ± 0 efficiency of *kasOp** insertion upstream of *doxA* and *dnrO* deletion in pCAP01-*epi*, respectively (Supplementary S12C, D). However, a high frequency of colonies containing the unedited and the edited plasmids (mixed plasmids) was observed in the editing of pCAP01-*epi*, particularly for insertion of *kasOp** upstream of *doxA* (Supplementary Fig. S12C). This phenomenon was not found in the iCASRED-based editing of NP BGCs cloned in the single-copy BAC plasmid. We reasoned that it is possibly ascribed to the decreased iCASRED-based DNA cleavage of the high-copy plasmids and thereby resulting in its lower counter-selection ability of strains with the unedited plasmids. The colonies with mixed plasmids could be converted to colonies with only edited plasmids with 100 % efficiency by subculture one time on LB agar plates (Supplementary Fig. S12E). The correct target editing was further confirmed by PCR product sequencing (data not shown).

3.8. iCASRED-based iterative BGC editing

In general, several genes or sites require to be edited for BGC refactoring. Therefore, we checked the efficiency of iterative editing, and two edited BAC plasmids, including pCL01-*omil*:*milF* and pCL01*int32-spi* (Fig. 6A–C), were tested as the starting plasmids for two-round iterative editing. In the first round, the competent cells of BL23/pCL01-*omil*:*milF* and BL23/pCL01*int32-spi* were prepared and electroporated with the editing plasmid pTarget-$sg^{milR\text{-}kasOp*}$/HA (for *milR* promoter replacement) and pTarget-sg^{spnK}/HA (for *spnK* deletion), respectively. The positive colonies harboring the expected editing were analyzed by colony PCR and confirmed by DNA sequencing (Supplementary Fig. S13). We achieved the efficiency of approximately 86.7 % ± 3.8 % and 84.4 % ± 6.7 %, respectively (Fig. 6B–D). After editing plasmid curing, the strains with the corresponding edited BAC

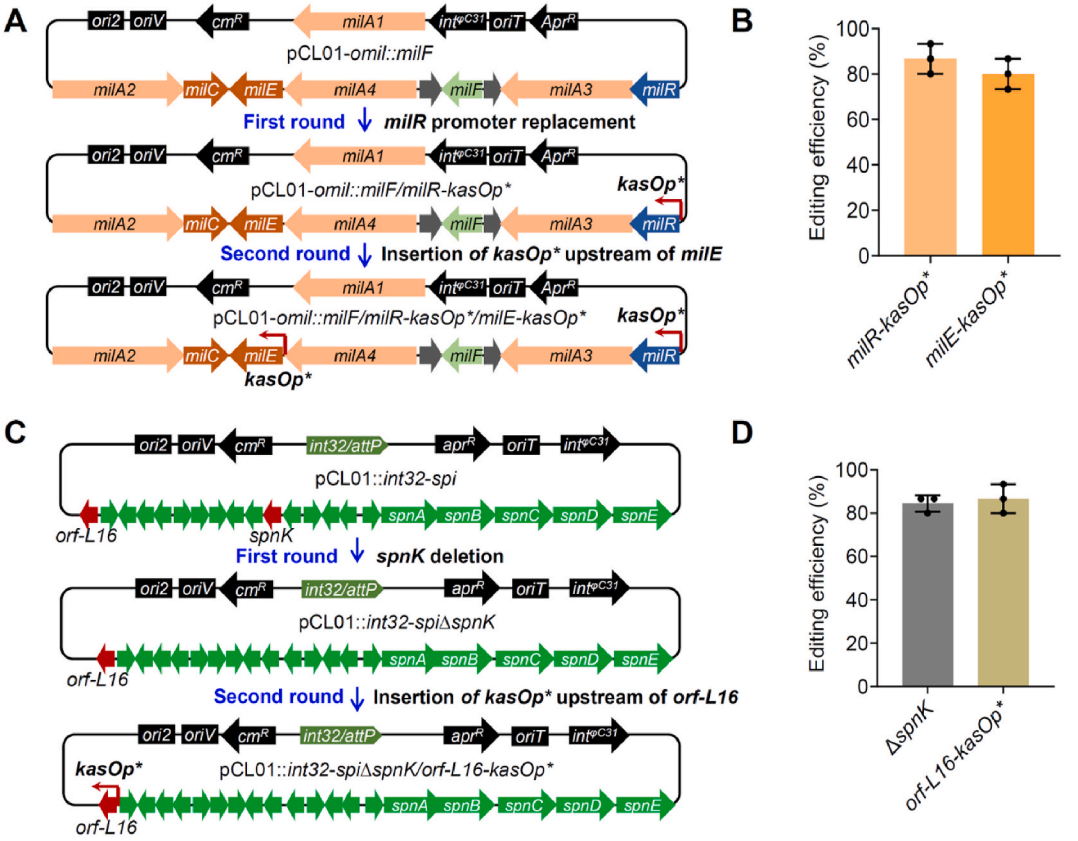

Fig. 6. iCASRED-based two-round iterative BGC editing in BL23. (**A**) The process of iCASRED-based two-round iterative editing of pCL01-*omil*:*milF* and the schematic maps of the corresponding edited plasmids. First round: *milR* promoter replacement by *kasOp**; Second round: insertion of *kasOp** promoter upstream of *milE*. (**B**) Efficiencies of each round of iCASRED-based iterative editing of pCL01-*omil*:*milF*. The error bars represent the standard deviations of the editing efficiencies from three independent experiments. (**C**) The process of iCASRED-based two-round iterative editing of pCL01*int32-spi* and the schematic maps of the corresponding edited plasmids. First round: *spnK* deletion; Second round: insertion of *kasOp** upstream of *orf-L16*. (**D**) Efficiencies of each round of iCASRED-based iterative editing of pCL01*int32-spi*. The error bars represent the standard deviations of the editing efficiencies from three independent experiments.

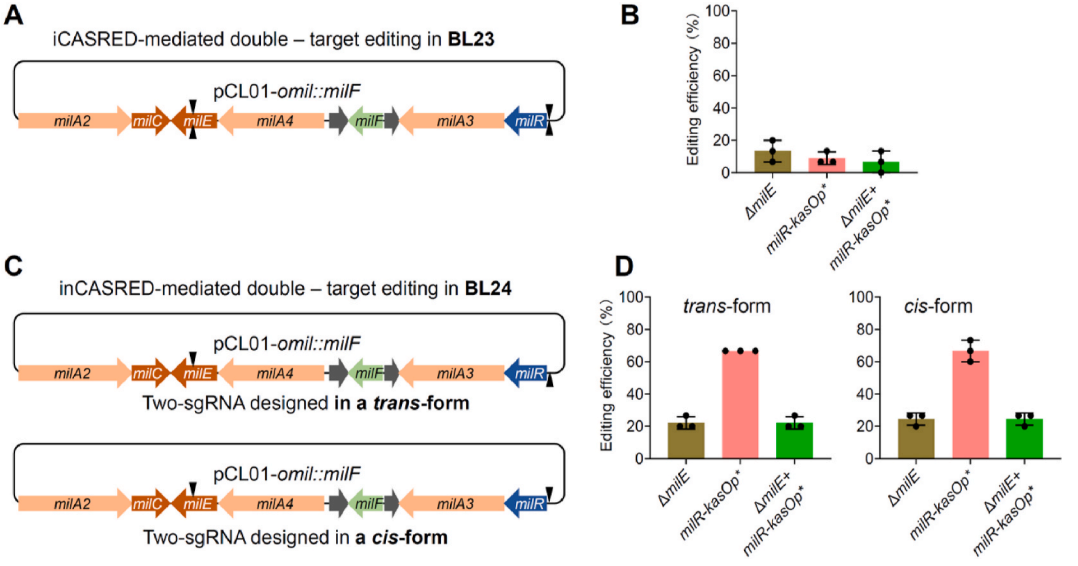

Fig. 7. iCASRED or inCASRED-based double-target editing of NP BGC in *E. coli*. (**A**) The schematic map of pCL01-*omil::milF* subjected to iCASRED-based double-target editing. Two target genes and the Cas9 cleavage sites (double-stranded cleavage, showed by black arrows) are as indicated. (**B**) Efficiencies of iCASRED-based double-target editing of pCL01-*omil*:*milF*. The efficiencies of only single-target editing are also indicated. The error bars represent the standard deviations of the editing efficiencies from three independent experiments. (**C**) The schematic map of pCL01-*omil::milF* subjected to inCASRED-based double-target editing with two sgRNAs designed in a *trans*- or *cis*-form. Two target genes and the nCas9 cleavage sites (single-stranded cleavage, showed by black arrows) are as indicated. (**D**) Efficiencies of inCASRED-based double-target editing of pCL01-*omil*:*milF*. The efficiencies of single-target editing are also indicated. The error bars represent the standard deviations of the editing efficiencies from three independent experiments.

plasmid were further subjected to the second round of editing, and insertion of *kasOp** upstream of *milE* (in pCL01-*omil:milF:milR-kasOp**) and *orf-L16* (in pCL01*int32-spi*Δ*spnK*) were individually conducted. The editing efficiency was determined to be 80.0 % ± 6.7 % and 86.7 % ± 3.8 %, respectively (Fig. 6B–D). The above results clearly demonstrated that iCASRED in BL23 could enable easily iterative editing of large BGCs. For each round of BGC editing, apart from the time spent on editing plasmid construction, the entire process takes approximately 4 days (calculated from the moment we obtain the strain containing only the BAC plasmid), including competent cell preparation (1 day), editing plasmid transformation followed by colony PCR analysis (1 day), and plasmid curing (2 days, including IPTG induction overnight, streaking and screening on LB plates or in liquid medium) (Fig. 1).

3.9. iCASRED-mediated scarless double-target editing of NP BGCs

To determine whether iCASRED could be used for scarless multi-site editing of NP BGCs, we conducted simultaneous editing of both *milE* deletion and *milR* promoter replacement in pCL01-*omil* (Fig. 7A). The editing plasmid pTarget-sg^{milE}/HA-$sg^{milR\text{-}kasOp}$*/HA were constructed and electroporated into the competent cells of BL23/pCL01-*omil*. We showed that, under the same transformation condition, introduction of single-target editing plasmids (pTarget-sg^{milE}/HA and pTarget-$sg^{milR\text{-}kasOp}$*/HA) led to the formation of approximately 1860 and 2600 transformants, respectively (Fig. 4B); however, only 48–63 transformants were obtained for the double-target editing plasmid (Supplementary Fig. S14A). Colony PCR revealed that iCASRED-based editing achieved approximately 13.3 % ± 6.7 % efficiency of *milE* deletion and 8.8 % ± 3.9 % efficiency of promoter replacement of *milR*, and 6.6 % ± 6.6 % efficiency for simultaneous editing of both targets (Fig. 7B and Supplementary Fig. S14B), which was further confirmed by PCR product sequencing (data not shown). The results clearly indicated that, when targeting two targets simultaneously, the efficiencies of both editing plasmid transformation and BGC editing were drastically lower than those for editing single targets. It was reported that λRed-mediated recombination occurs at the replication fork and therefore requires ongoing replication [38,39]. We reasoned that two Cas9-induced DSBs resulted in the DNA fragment between two DSBs failure to replicate, thereby leading to the decreased ability of λRed-mediated repair.

To improve double-target editing efficiency, we attempted to employ nCas9 ($Cas9^{D10A}$) instead of Cas9, which only induces single-stranded breaks (SSBs) and the replication ability of the DNA between two cutting sites could be maintained. As the first step, the *Cas9* gene in BL23 was mutated to *nCas9* based on iCASRED-mediated genome editing and the engineered strain was named BL24. Then, using BL24 as the host, we conducted nCas9/λRed (inCASRED)-based simultaneous double-target editing of both *milE* deletion and *milR* promoter replacement (Fig. 7C). Two editing plasmids (pTargetn-sg^{milE}/HA-$sg^{milR\text{-}kasOp}$*/HA-*trans* and pTargetn-sg^{milE}/HA-$sg^{milR\text{-}kasOp}$*/HA-*cis*) harboring the transcription cassettes of two sgRNAs targeting two respective strand (*trans*) and the same strand (*cis*) were constructed and introduced into the competent cells of BL24. We showed that introduction of inCASRED-based editing plasmid resulted in the formation of approximately 450–750 colonies, which are approximately 10–11 times as that formed after introduction of iCASRED-based double-target editing plasmid, clearly indicating the lower toxicity of nCas9-induced SSBs to *E. coli*. Colony PCR revealed that when two sgRNAs were designed in *trans*-form, inCASRED achieved the efficiencies of 24.4 % ± 3.8 % and 66.7 % ± 0 % for the respective editing of *milE* and *milR* and an efficiency 24.4 % ± 3.8 % for simultaneous editing of both targets. When two sgRNAs were designed in *cis*-form, inCASRED achieved similar editing efficiencies, approximately 24.4 % ± 3.8 % and 68.9 % ± 6.7 % for the respective editing of *milE* and *milR* and an efficiency 22.2 % ± 3.8 % for simultaneous editing of both targets (Fig. 7D and Supplementary Figs. S14B and C). Similar results were obtained for simultaneous double-target editing, including *kasOp** insertion upstream of *milF* and *milR* promoter replacement. inCASRED could achieve approximately 24.4 % ± 3.8 % (*trans*) and 20 % ± 3.8 % (*cis*) efficiencies for simultaneous editing of both targets (Supplementary Fig. S15).

It is worth to note that a high frequency of the existence of colonies with both the unedited and the edited plasmids was observed for both single-target and simultaneous double-target editing in pCL01-*omil* (Supplementary Figs. S14 and S15). This point should be ascribed to the weak counter-selection ability of nCas9, which could only induced SSBs. The colonies with mixed plasmids can be converted to colonies with only edited plasmids with 100 % efficiency by subculture one time on LB agar plates (data not shown). In addition, we can clearly see two different sizes of colonies on the LB plates after editing plasmid transformation, and colony PCR analysis showed that the efficiencies of BGC editing in small colonies is significantly higher than that in big colonies (data not shown). This may be due to the relatively lower efficiency of repairing two DSBs simultaneously. We further showed that the editing plasmid pTargetn-sg^{milE}/HA-$sg^{milR\text{-}kasOp}$*/HA could be cured at approximately 90 % efficiency in BL24 after induction by IPTG and as a control, without IPTG induction, the editing plasmid could also be cured at an efficiency of 30 % (Supplementary Fig. S16).

3.10. Verification of the edited plasmids by restriction enzyme digestion and BGC expression in actinomycete hosts

To further verify the correctness of the recombinant plasmids with edited NP BGCs, plasmid restriction enzyme digestion and BGC expression in a heterologous or native host were conducted. Firstly, restriction enzyme digestion of the edited plasmids were performed and the DNA band profiles were compared with the simulated agarose electrophoresis by SnapGene. Here, six edited plasmids with different target editing as indicated in Supplementary Fig. S17 were tested and digested with three different enzymes or enzyme combination (*Xho*I, *Nde*I/*Eco*RV, and *Bam*HI). For each edited plasmid, three parallel recombinant plasmids (biological replicates) were isolated from the cultures of three randomly selected colonies after editing plasmid curing. We showed that all three biological replicates of five BAC- or pCAP01-based recombinant plasmids produced expected bands after enzyme treatment, which are identical to those obtained from simulated agarose electrophoresis. However, in one of three parallel edited BAC plasmid, pCL01-*omil/milR-kasOp**, showed a false DNA band profile, suggesting that there exists a certain degree of false or non-specific editing of the tested BGCs (Supplementary Fig. S17). Therefore, it is necessary to perform enzyme digestion validation of the obtained plasmids before proceeding to the next step.

Subsequently, two edited pCL01-*omil* (including pCL01-*omil::milF* and pCL01-*omil::milF/milR-kasOp**) and two edited pCL01*int32-spi* (including pCL01*int32-spi*Δ*spnK* and pCL01*int32-spi*Δ*spnK/L16-kasOp**) were functional characterized by expression in a heterologous host and a native spinosyns-producing strain, respectively. The 5-oxo-milbemycins BGC in pCL01-*omil* was derived from milbemycins BGC by deleting the *milF* gene, which encodes a C5-ketoreductase and is responsible for the reduction of C5-keto groups of milbemycins (the main components, milbemycin A3/A4) [40,41]. Insertion of *milF* will result in the production of milbemycins, but not 5-oxo-milbemycins (Fig. 8A). MilR acts a pathway-specific activator of milbemycin biosynthesis and its overexpression would result in increased milbemycin production [42]. The edited BAC plasmids, including pCL01-*omil::milF* and pCL01-*omil::milF/milR-kasOp**, were introduced into a *Streptomyces avermitilis* host with the deletion of the avermectin BGC (Δ*ave*). HPLC analysis of fermentation cultures revealed that, compared with the Δ*ave* strain harboring the starting plasmid pCL01-*omil* produced 5-oxo-milbemycin A3/A4, introduction of either pCL01-*omil::milF* or pCL01-*omil::milF/milR-kasOp** into Δ*ave* resulted in milbemycin A3/A4 production (Fig. 8B). We also found that identical to the function of MilR, the engineered strain with pCL01-*omil::milF/milR-kasOp** produced 25.7 % ± 5.2 % higher milbemycin A3/A4 levels than that with pCL01-*omil::*

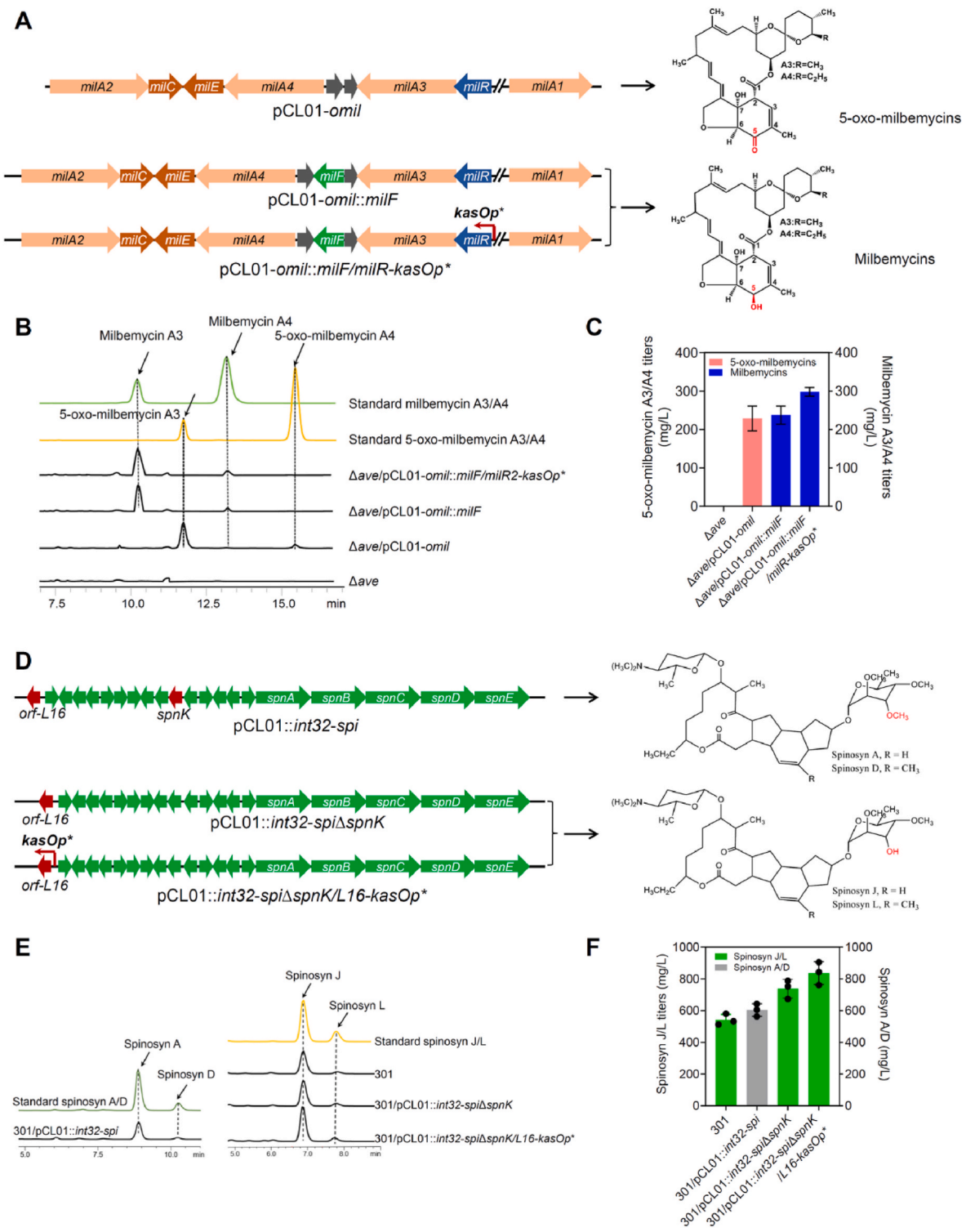

Fig. 8. Functional identification of the edited BGCs by integrative expression in a heterologous or a native host. (**A**) Schematic diagram of the pCL01 plasmids with the respective cloning of 5-oxo-milbemycin BGC and its derived BGCs obtained by iCASRED-based editing. The structure of chemical compounds that produced by these BGCs were as indicated. (**B**) HPLC analysis of fermentation cultures of the engineered *S. avermitilis* Δ*ave* after introduction of pCL01-*omil*, pCL01-*omil::milF*, and pCL01-*omil::milF/milR-kasOp**, respectively. The standards of milbemycin A3/A4 and 5-oxo-milbemycin A3/A4 (the main components of milbemycins and 5-oxo-milbemycins) were provided. Fermentation cultures were collected after growth for 12 days. (**C**) The titers of milbemycin A3/A4 and 5-oxo-milbemycin A3/A4 produced by the engineered heterologous host *S. avermitilis* Δ*ave* after introduction of pCL01-*omil*, pCL01-*omil::milF*, and pCL01-*omil::milF/milR-kasOp**, respectively. The error bars represent the standard deviations of the results from three independent experiments. (**D**) Schematic diagram of the pCL01*int32* plasmids with the respective cloning of spinosyn A/D BGC and its derived BGCs obtained by iCASRED-based editing. The structure of chemical compounds that produced by these BGCs were as indicated. (**E**) HPLC analysis of fermentation cultures of the engineered *S. spinosa* 301 after introduction of pCL01*int32-spi*, pCL01*int32-spi*Δ*spnK*, and pCL01*int32-spi*Δ*spnK/L16-kasOp**, respectively. The standards of spinosyn A/D and spinosyn J/L were provided. Fermentation cultures were collected after growth for 10 days. (**F**) The titers of spinosyn A/D and spinosyn J/L produced by the engineered *S. spinosa* 301 after introduction of pCL01*int32-spi*, pCL01*int32-spi*Δ*spnK*, and pCL01*int32-spi*Δ*spnK/L16-kasOp**, respectively. The error bars represent the standard deviations of the results from three independent experiments.

milF (Fig. 8C).

The edited pCL01*int32-spi*, including pCL01*int32-spi*Δ*spnK* and pCL01*int32-spi*Δ*spnK/L16-kasOp**, were transferred into the spinosyn J/L-producing strain *S. spinosa* 301. The *spnK* gene encodes a 3′-*O*-methyltransferase, which catalyzes the methylation of the 3′-hydroxyl (3′-O-methylation) of rhamnose [43]. Its deletion resulted in the formation of spinosyn J/L instead of spinosyn A/D (Fig. 8D). *orf-L16*, which encodes a LysR-family regulator, functions as an activator for spinosyns biosynthesis [44]. Its overexpression will increase spinosyns production. We showed that introduction of the control plasmid pCL01*int32-spi* (containing the spinosyn A/D BGC) into 301 resulted in the production of spinosyn A/D but not spinosyn J/L (Fig. 8E). This results indicates that the product of one copy of *spnK* provided in pCL01*int32-spi* is sufficient to catalyze 3′-O-methylation of rhamnose, thereby leading to the formation of only spinosyn A/D. When the edited plasmids, including pCL01*int32-spi*Δ*spnK* and pCL01*int32-spi*Δ*spnK/L16-kasOp**, were introduced into 301, spinosyn J/L titers were increased by 36.3 % ± 4.5 % and 54.5 % ± 6.9 %, respectively, as compared with the parental strain). Identical to the function of Orf-L16 [44], the engineered 301 strain with pCL01*int32-spi*Δ*spnK/L16-kasOp** produced a slightly higher spinosyn J/L titers than that with pCL01*int32-spi*Δ*spnK* (Fig. 8F).

The results from restriction enzyme digestion and BGC expression in actinomycete hosts clearly demonstrated that iCASRED-based editing has high specificity, thereby enabling the sequence integrity and correctness of the edited gene clusters.

4. Discussion

In this study, we established an effective scarless DNA editing tool (iCASRED) for refactoring NP BGCs in *E. coli* BL23 with chromosomal integration of the *Cas9* gene and the λRed system, combined with *recA* deletion and simultaneous insertion of the inducible transcription module of sgRNA (sg^T) targeting the editing plasmid. iCASRED in BL23 could achieve high-efficiency editing of single targets in BGCs cloned either in single-copy BAC plasmids or high-copy plasmids (e.g. pCAP01). The editing types include DNA deletions, insertions, and promoter replacements. iCASRED in BL23 enabled simultaneous scarless double-target editing with an efficiency of approximately 6.6 % ± 6.6 %, which could be increased to 24.4 % ± 3.8 % by replacement of Cas9 by nCas9. Compared with the currently developed *in vivo* BGC editing tools in *E. coli* [9,16–19,23] and yeast [18,20–22], which would leave at least one selection marker or DNA scars (such as FRT sites) in the edited BGCs and thereby possibly affect BGCs function, our tool could achieve efficient scarless BGC editing for single-and double-target. In addition, owing to the integration of the *Cas9* (or nCas9)/λRed expression cassettes into the *E. coli* genome, the operation process of our tool is simple and convenient, which only need the construction and transformation of an all-in-one editing plasmid harboring the specific sgRNAs and repair templates. It is time-saving, which takes only 4 days for each round of editing. Importantly, our tool enabled fast and efficient iterative BGC editing due to high-efficiency curing of the editing plasmids, which can partially compensate for the low efficiency of multi-target BGC editing. Collectively, our work provides a simple and effective NP BGC editing platform, which may facilitate the activation of silent BGCs for the discovery of novel NPs and strain improvement for high-yield of target compounds.

The existing *in vivo* gene cluster editing technology in *E. coli* uses linear fragments as DNA templates for BGC editing [9,16–19,23]. Due to the degradation of linear DNA by intracellular nucleases (e.g. RecBCD exonuclease) after entering the cell, a high concentration of DNA templates is required. In addition, to improve editing efficiency, they need to use at least one screening marker (e.g. antibiotic resistance genes) or combined with *ccdB* counterselection [19]. The repair templates in our tool comes from a replicative plasmid with *pMB1* origin (copy number 15–20) [24], which continuously replicates and provides DNA templates after entering the cell. This may be the reason why our tool can achieve high-efficiency editing of single targets in the absence of selection markers. It can be imagined that using higher copy vectors for the construction of editing plasmids may further improve the efficiency of scarless gene cluster editing, particularly for multiplexed editing.

A main limitation of out tools is the low efficiency for double-target editing (6.6 % ± 6.6 % of iCASRED and 24.4 % ± 3.8 % of inCASRED), which needs to be addressed. This is also the reason why we did not conduct simultaneous editing of three or more targets. In our study, we observed a high leakage transcription of sg^T targeting the editing plasmids (Supplementary Figs. S4 and S16), which may result in the high-level degradation of editing plasmids, thereby leading to reduced supply of repair templates and accordingly decreased double-target editing efficiency. This point may be addressed by controlling sg^T expression using a stricter inducible promoter.

It is worth to note that a low proportion of unexpected PCR products in colony PCR analysis for iCASRED-based editing of tested genes, including *milE* deletion in pCL01-*omil* and *kasO*p* promoter insertion upstream of *orf-L16* in pCL01-*spi*. To explore the possible causes of this phenomenon, we sequenced eight PCR products from three independent analysis (insertion of *kasOp** upstream of *orf-L16*) with DNA sizes obviously smaller than that expected (Supplementary Fig. S18). We showed that all eight sequenced PCR products contained different sizes of DNA deletions upstream and downstream of the designed sgRNA targeting site (142–276 bp and 72–347 bp, respectively) and there exist 2–12 bp of microhomology sequences at the deletion junctions. We reasoned that the formation of unexpected smaller PCR products should be ascribed to DSB repair mediated by microhomology DNA-induced alternative end-joining mechanism (A-EJ) involving RecBCD-based end resection as reported previously [45]. In our iCASRED tool, Gam protein (γ) from the λRed system functions as an inhibitor of *E. coli* RecBCD [46]. The above phenomenon clearly suggested that in the BL23 chassis, the expression of Gam needs to be enhanced and thereby further reduces the activity of RecBCD, which may be helpful for iCASRED-based high-specificity editing.

CRediT authorship contribution statement

Guosong Zheng: Writing – original draft, Methodology, Investigation, Data curation. **Jiafeng Xu:** Methodology, Investigation, Data curation. **Hewei Liu:** Methodology, Investigation, Data curation. **Huimin Hua:** Methodology, Data curation. **Andrei A. Zimin:** Writing – review & editing, Software. **Wenfang Wang:** Writing – review & editing, Project administration, Conceptualization. **Yinhua Lu:** Writing – review & editing, Writing – original draft, Supervision, Project administration, Funding acquisition, Conceptualization.

Data availability

The data supporting the findings of our study are available in the Supplementary Data of this manuscript, including supplementary materials and methods, strains and plasmids used or constructed (Supplementary Table S1), primer sequences (Supplementary Table S2), and supplementary figures (S1-S18).

Funding

This work was supported by the National Key Research and Development Program (2019YFA0905400 to Y.L.) and the National Natural Science Foundation of China (32270095 to Y. L.).

Declaration of competing interest

The authors declare that they have no known competing financial interests or personal relationships that could have appeared to influence the work reported in this paper.

Acknowledgements

We hope to express our thanks to Prof. Sheng Yang from CAS Center for Excellence in Molecular Plant Sciences, Chinese Academy of Sciences for kindly providing the plasmids of pTargetF-*cat* and pCas.

Appendix A. Supplementary data

Supplementary data to this article can be found online at https://doi.org/10.1016/j.synbio.2025.03.008.

References

[1] Demain AL. Importance of microbial natural products and the need to revitalize their discovery. J Ind Microbiol Biotechnol 2014;41:185–201.
[2] Giddings LA, Newman DJ. Microbial natural products: molecular blueprints for antitumor drugs. J Ind Microbiol Biotechnol 2013;40:1181–210.
[3] Nett M, Ikeda H, Moore BS. Genomic basis for natural product biosynthetic diversity in the actinomycetes. Nat Prod Rep 2009;26:1362–84.
[4] Kalkreuter E, Pan G, Cepeda AJ, Shen B. Targeting bacterial genomes for natural product discovery. Trends Pharmacol Sci 2020;41:13–26.
[5] Shen B. A new Golden age of natural products drug discovery. Cell 2015;163:1297–300.
[6] Kang HS, Kim ES. Recent advances in heterologous expression of natural product biosynthetic gene clusters in *Streptomyces* hosts. Curr Opin Biotechnol 2021;69:118–27.
[7] Nepal KK, Streptomycetes Wang G. Surrogate hosts for the genetic manipulation of biosynthetic gene clusters and production of natural products. Biotechnol Adv 2019;37:1–20.
[8] Lee N, Hwang S, Lee Y, Cho S, Palsson B, Cho BK. Synthetic biology tools for novel secondary metabolite discovery in *Streptomyces*. J Microbiol Biotechnol 2019;29:667–86.
[9] Alam K, Hao J, Zhang Y, Li A. Synthetic biology-inspired strategies and tools for engineering of microbial natural product biosynthetic pathways. Biotechnol Adv 2021;49:107759.
[10] Li L, Maclntyre LW, Brady SF. Refactoring biosynthetic gene clusters for heterologous production of microbial natural products. Curr Opin Biotechnol 2021;69:145–52.
[11] Tao W, Yang A, Deng Z, Sun Y. CRISPR/Cas9-based editing of *Streptomyces* for discovery, characterization, and production of natural products. Front Microbiol 2018;9:1660.
[12] Abbasi MN, Fu J, Bian X, Wang H, Zhang Y, Li A. Recombineering for genetic engineering of natural product biosynthetic pathways. Trends Biotechnol 2020;38:715–28.
[13] Liu Y, Tao W, Wen S, Li Z, Yang A, Deng Z, Sun Y. *In vitro* CRISPR/Cas9 system for efficient targeted DNA editing. mBio 2015;6:e01714. 01715.
[14] Li L, Zheng G, Chen J, Ge M, Jiang W, Lu Y. Multiplexed site-specific genome engineering for overproducing bioactive secondary metabolites in actinomycetes. Metab Eng 2017;40:80–92.
[15] Kudo K, Hashimoto T, Hashimoto J, Kozone I, Kagaya N, Ueoka R, Nishimura T, Komatsu M, Suenaga H, Ikeda H, et al. *In vitro* Cas9-assisted editing of modular polyketide synthase genes to produce desired natural product derivatives. Nat Commun 2020;11:4022.
[16] Muyrers JP, Zhang Y, Testa G, Stewart AF. Rapid modification of bacterial artificial chromosomes by ET-recombination. Nucleic Acids Res 1999;27:1555–7.
[17] Nguyen KT, Ritz D, Gu JQ, Alexander D, Chu M, Miao V, Brian P, Baltz RH. Combinatorial biosynthesis of novel antibiotics related to daptomycin. Proc Natl Acad Sci U S A 2006;103:17462–7.
[18] Yamanaka K, Reynolds KA, Kersten RD, Ryan KS, Gonzalez DJ, Nizet V, Dorrestein PC, Moore BS. Direct cloning and refactoring of a silent lipopeptide biosynthetic gene cluster yields the antibiotic taromycin A. Proc Natl Acad Sci U S A 2014;111:1957–62.
[19] Song C, Luan J, Li R, Jiang C, Hou Y, Cui Q, Cui T, Tan L, Ma Z, Tang YJ, et al. RedEx: a method for seamless DNA insertion and deletion in large multimodular polyketide synthase gene clusters. Nucleic Acids Res 2020;48:e130.
[20] Montiel D, Kang HS, Chang FY, Charlop-Powers Z, Brady SF. Yeast homologous recombination-based promoter engineering for the activation of silent natural product biosynthetic gene clusters. Proc Natl Acad Sci U S A 2015;112:8953–8.
[21] Kang HS, Charlop-Powers Z, Brady SF. Multiplexed CRISPR/Cas9- and TAR-mediated promoter engineering of natural product biosynthetic gene clusters in yeast. ACS Synth Biol 2016;5:1002–10.
[22] Kim H, Ji CH, Je HW, Kim JP, mpCRISTAR Kang HS. Multiple plasmid approach for CRISPR/Cas9 and TAR-mediated multiplexed refactoring of natural product biosynthetic gene clusters. ACS Synth Biol 2020;9:175–80.
[23] He F, Liu X, Tang M, Wang H, Wu Y, Liang S. CRISETR: an efficient technology for multiplexed refactoring of biosynthetic gene clusters. Nucleic Acids Res 2024;52:11378–93.
[24] Jiang Y, Chen B, Duan C, Sun B, Yang J, Yang S. Multigene editing in the *Escherichia coli* genome via the CRISPR-Cas9 system. Appl Environ Microbiol 2015;81:2506–14.
[25] Li L, Wei K, Liu X, Wu Y, Zheng G, Chen S, Jiang W, Lu Y. aMSGE: advanced multiplex site-specific genome engineering with orthogonal modular recombinases in actinomycetes. Metab Eng 2019;52:153–67.
[26] Lee NC, Larionov V, Kouprina N. Highly efficient CRISPR/Cas9-mediated TAR cloning of genes and chromosomal loci from complex genomes in yeast. Nucleic Acids Res 2015;43:e55.
[27] Posfai G, Plunkett 3rd G, Feher T, Frisch D, Keil GM, Umenhoffer K, Kolisnychenko V, Stahl B, Sharma SS, de Arruda M, et al. Emergent properties of reduced-genome *Escherichia coli*. Science 2006;312:1044–6.
[28] Huang H, Zheng G, Jiang W, Hu H, Lu Y. One-step high-efficiency CRISPR/Cas9-mediated genome editing in *Streptomyces*. Acta Biochim Biophys Sin 2015;47:231–43.
[29] Zou X, Xiao X, Mo Z, Ge Y, Jiang X, Huang R, Li M, Deng Z, Chen S, Wang L, et al. Systematic strategies for developing phage resistant *Escherichia coli* strains. Nat Commun 2022;13:4491.
[30] Hang X, Zeng Q, Zeng L, Jia J, Bi H. Functional replacement of the BioC and BioH proteins of *Escherichia coli* biotin precursor biosynthesis by *Ehrlichia chaffeensis* novel proteins. Curr Microbiol 2019;76:626–36.
[31] Lim CJ, Geraghty D, Fuchs JA. Cloning and nucleotide sequence of the *trxA* gene of *Escherichia coli* K-12. J Bacteriol 1985;163:311–6.
[32] Wang W, Li X, Wang J, Xiang S, Feng X, Yang K. An engineered strong promoter for streptomycetes. Appl Environ Microbiol 2013;79:4484–92.
[33] Zurcher JF, Kleefeldt AA, Funke LFH, Birnbaum J, Fredens J, Grazioli S, Liu KC, Spinck M, Petris G, Murat P, et al. Continuous synthesis of *E. coli* genome sections and Mb-scale human DNA assembly. Nature 2023;619:555–62.
[34] Chen J, Xia H, Dang F, Xu Q, Li W, Qin Z. Characterization of the chromosomal integration of *Saccharopolyspora* plasmid pCM32 and its application to improve production of spinosyn in *Saccharopolyspora spinosa*. Appl Microbiol Biotechnol 2015;99:10141–9.
[35] Park W, Woo JK, Shin J, nonG Oh KB. A constituent of the nonactin biosynthetic gene cluster, regulates nocardamine synthesis in *Streptomyces albus* J1074. Biochem Biophys Res Commun 2017;490:664–9.
[36] Iqbal HA, Low-Beinart L, Obiajulu JU, Brady SF. Natural product discovery through improved functional metagenomics in *Streptomyces*. J Am Chem Soc 2016;138:9341–4.
[37] Blodgett JA, Zhang JK, Metcalf WW. Molecular cloning, sequence analysis, and heterologous expression of the phosphinothricin tripeptide biosynthetic gene cluster from *Streptomyces viridochromogenes* DSM 40736. Antimicrob Agents Chemother 2005;49:230–40.
[38] Maresca M, Erler A, Fu J, Friedrich A, Zhang Y, Stewart AF. Single-stranded heteroduplex intermediates in lambda Red homologous recombination. BMC Mol Biol 2010;11:54.
[39] Ellis HM, Yu D, DiTizio T, Court DL. High efficiency mutagenesis, repair, and engineering of chromosomal DNA using single-stranded oligonucleotides. Proc Natl Acad Sci U S A 2001;98:6742–6.
[40] Wang XJ, Wang CQ, Sun XL, Xiang WS. 5-ketoreductase from *Streptomyces bingchengensis*: overexpression and preliminary characterization. Biotechnol Lett 2010;32:1497–502.
[41] Wang HY, Zhang J, Zhang YJ, Zhang B, Liu CX, He HR, Wang XJ, Xiang WS. Combined application of plasma mutagenesis and gene engineering leads to 5-oxomilbemycins A3/A4 as main components from *Streptomyces bingchenggensis*. Appl Microbiol Biotechnol 2014;98:9703–12.
[42] Zhang Y, He H, Liu H, Wang H, Wang X, Xiang W. Characterization of a pathway-specific activator of milbemycin biosynthesis and improved milbemycin production by its overexpression in *Streptomyces bingchenggensis*. Microb Cell Fact 2016;15:152.
[43] Kim HJ, White-Phillip JA, Ogasawara Y, Shin N, Isiorho EA, Liu HW. Biosynthesis of spinosyn in *Saccharopolyspora spinosa*: synthesis of permethylated rhamnose and characterization of the functions of SpnH, SpnI, and SpnK. J Am Chem Soc 2010;132:2901–3.
[44] Mu X, Lei R, Yan S, Deng Z, Liu R, Liu T. The LysR family transcriptional regulator ORF-L16 regulates spinosad biosynthesis in *Saccharopolyspora spinosa*. Synth Syst Biotechnol 2024;9:609–17.
[45] Chayot R, Montagne B, Mazel D, Ricchetti M. An end-joining repair mechanism in *Escherichia coli*. Proc Natl Acad Sci U S A 2010;107:2141–6.
[46] Murphy KC. Lambda Gam protein inhibits the helicase and chi-stimulated recombination activities of *Escherichia coli* RecBCD enzyme. J Bacteriol 1991;173:5808–21.